

# Double-exponential curve fitting of isometric relaxation: a new measure for myocardial lusitropism

KOUICHI TAMIYA, TOSHIYUKI BEPPU, AND KAZUAKI ISHIHARA

*Departments of Surgical Science and Pediatric Cardiovascular Surgery,  
The Heart Institute of Japan, Tokyo Women's Medical College, Tokyo 162, Japan*

**Tamiya, Kouichi, Toshiyuki Beppu, and Kazuaki Ishihara.** Double-exponential curve fitting of isometric relaxation: a new measure for myocardial lusitropism. *Am. J. Physiol.* 269 (*Heart Circ. Physiol.* 38): H393–H406, 1995.—New indexes for evaluation of isometric myocardial relaxation were proposed. In fully isometric and physiologically sequenced twitches, the time course of isometric force decline fitted well with Gompertz's double-exponential curve ( $r \geq 0.9995$ ). We conformed the original equation to suit myocardial mechanics, i.e.,  $F(t) = \gamma_0 - \gamma \cdot \exp[-\alpha \cdot \exp(-\beta t)]$  ( $t = 1, 2, \dots, n$ ), where  $F(t)$  denotes force as a function of time  $t$ . The  $\gamma_0$  and  $\gamma$  relate to upper asymptote and force amplitude, respectively. Phase-plane analysis of  $F(t)$  revealed that  $\alpha$  [ $3.56 \pm 0.67$  (SD)] related to the phasic delay of relaxation onset but did not affect the  $F(t)$  vs.  $dF(t)/dt$  relation. The  $\beta$  ( $0.127 \pm 0.021$ ) and  $\gamma$  were linearly related to negative  $dF(t)/dt_{\max}$ ; however, the terminal slope of the phase-plane diagram was governed by  $\beta$  alone. The  $\tau_\beta$  ( $0.081 \pm 0.017$  s), a reciprocal of  $\beta$  multiplied by sampling time, was practically independent of preload, total load, and muscle shortening. In isometric twitches,  $\tau_\beta$  was substantially decreased by global ischemia, isoproterenol, and  $\text{CaCl}_2$  but increased by reperfusion. The  $\alpha$  was independent of inotropic interventions but fell significantly during ischemia and was increased by reperfusion.

isometric indexes of relaxation; time constant of exponential isometric force decay; lusitropic state of myocardium; blood-perfused canine papillary muscle

ALTHOUGH MECHANICAL PROPERTIES of relaxing myocardium have been studied in the whole ventricle in situ and in the isolated myocardium in vitro (2), no comprehensive parametric description of isometric force decay that is feasible throughout the entire isometric relaxation phase has been derived. An empirical global formula utilizing nonlinear curve fitting was proposed (10); however, its utility was confined within fully isometric twitches. From the viewpoint of feasibility of the muscle mechanics to the ventricular dynamics, investigation on the isometric relaxation combined with muscle shortening is indispensable. In the whole ventricle, monoexponential curve fitting just after the peak negative time derivative ( $dP/dt$ ) of left ventricular pressure has widely been accepted as an evaluation method of relaxation characteristics in ejecting and nonejecting ventricles (4, 8, 18). The exponential curve fitting has an advantage that relaxation characteristics could be represented by a single parameter, i.e., the time constant  $\tau$ . In the isometric twitch and the physiologically sequenced relaxation, a distinct inflection point appears amid the time course of isometric force decay (5–6, 9, 14–16) as well as in the left ventricular pressure fall. A recent study by Sys and Brutsaert (14), which advocated utility of the phase-plane analysis in the assessment of myocardial

lusitropism, showed that the isometric force decay in their phase-plane diagram was curvilinear, even at its terminal point in the isometric twitch and in the physiologically sequenced relaxation. If a part of the isometric force decay was exponential, a portion of the phase-plane diagram should be rectilinear. Sys and Brutsaert clearly stated that the force decline could not be characterized as an exponential function (or by a time constant). In the physiologically sequenced contraction, the fact that the isotonic shortening velocity gradually approaches zero at the end of muscle shortening strongly suggests that the isometric relaxation starts with zero slope at its very onset. In addition, it is unlikely that the muscle suddenly changes its mechanical property at the time of peak rate of force decay, even though the force decline after peak negative  $dF(t)/dt$ , where  $F(t)$  denotes force as a function of time  $t$ , closely adheres to the exponential function. These findings and considerations convinced us that the isometric force decline in the physiologically sequenced relaxation takes place convexly at first, then concavely (reversed S shape), whether or not the muscle shortens.

Recently, we noticed that the double-exponential function, which had been formulated by Gompertz in 1825, readily expressed the entire time course of isovolumic pressure fall in the ejecting ventricle. In the present report, we introduce double-exponential curve fitting as a tool for evaluation of myocardial lusitropism during the isometric relaxation phase. In this evaluation method, two parameters of the double-exponential function,  $\alpha$  and  $\beta$ , independently characterize two aspects of relaxation:  $\alpha$  relates to the phasic delay of relaxation onset, and  $\beta$  principally relates to the rate of force decay. In this report, the new index  $\tau_\beta$  (a reciprocal of  $\beta$  multiplied by the sampling interval) is compared with the conventional time constant  $\tau$ , which is derived from the conventional exponential curve fitting of best fit, in the blood-perfused canine papillary muscle preparation. The current study also aimed to assess 1) the robustness of  $\tau_\beta$  against variations of preload, afterload, and extent of muscle shortening in the physiologically sequenced isometric relaxation and 2) the effect of isoproterenol,  $\text{CaCl}_2$ , global ischemia, and subsequent reperfusion on  $\alpha$  and  $\tau_\beta$  in fully isometric twitches.

## METHODS

Preparation of the specimen papillary muscle and the blood donor dog is basically as reported by Endoh and Hashimoto (3) in 1970. Briefly, we used two anesthetized dogs for each experiment: one was used for a specimen papillary muscle and the other as a blood donor dog. Care of the animals conformed to the recommendations of the Helsinki Declaration, and the study was conducted in accordance with the "Guide for the

Care and Use of Laboratory Animals" (NIH Publ. 85-23, revised 1985). After pentobarbital sodium (30-45 mg/kg iv) anesthesia, the heart of the former dog was excised and immediately plunged into cold saline at 4°C. The ventricular septum was excised, and the left anterior descending artery was cut open. While spontaneous contraction was inhibited in chilled saline, a fine polyvinyl cannula was inserted into the anterior septal artery via the left anterior descending artery. Then the muscle was perfused with warm arterial blood drawn from the heparinized blood donor dog at a regulated pressure of 120 mmHg (16 kPa) with use of a pressure servo-controlled blood pump. The temperature of the blood and the specimen muscle was maintained at 37°C with a thermostat bath and water jackets around the muscle and blood circuit. The venous blood returning via the thebesian vein from the preparation was corrected and returned to the blood donor dog via the external jugular vein. The base of the muscle was anchored to an acrylic resin board with several silk sutures, and the upper end (chorda tendinea) was connected to a strain gauge force transducer with a short segment of silk thread. Figure 1 shows the experimental setup, which is basically as described in our previous report (15), except the current setup employs a combination of an electromagnetic torque generator (a pen motor) and a transconductance amplifier instead of a counterweight. The total compliance of the lever system while the isotonic bar was locked (isometric mode) was 0.5  $\mu\text{m}/\text{mN}$ . The equivalent moving mass during the isotonic mode, measured at the tip of the lever by the free oscillation method (16), was 330 mg. Muscle force and muscle length, measured with a strain gauge force transducer and a differential transformer integrated in the pen motor, were inputted to an antialiasing filter bank (4th-order Cauer filter, 42 dB/oct, 50-Hz cutoff, model SR-4FL, NF Block, Yokohama, Japan) and digitized with a 12-bit analog-to-digital converter (model PCI-601W, Burr Brown, Tucson, AZ) at a sampling rate of 100 Hz/channel and stored in the IBM PS/2 computer through the DMA channel.

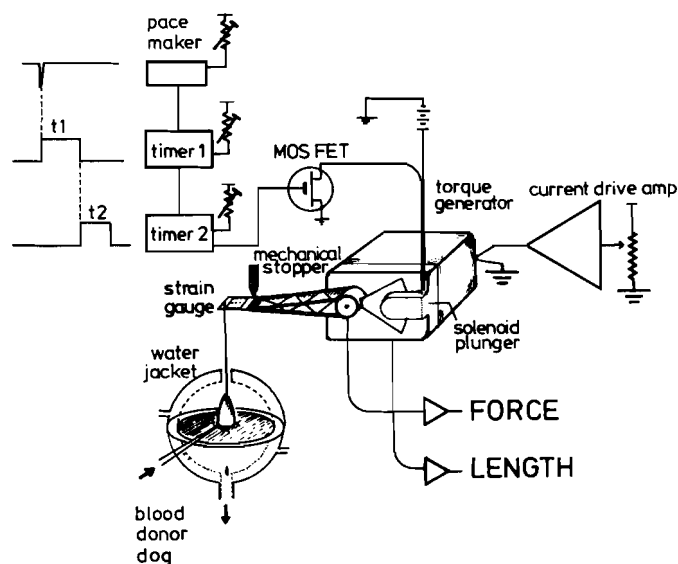


Fig. 1. Experimental setup. A solenoid plunger for muscle length clamp was installed on aluminum base of torque generator (pen motor). A muscle stimulator pulse triggers timer 1. Downward edge of timer 1 output triggers timer 2 in sequence. Hence, lever was locked by solenoid plunger at a desired instant (adjusted by  $t_1$ ) for a desired duration (controlled by  $t_2$ ). Variable power source of regulated current (transconductance amplifier) provides a predetermined constant current for moving coil during muscle shortening. MOS FET, metal oxide semiconductor field effect transistor.

### Data Processing

The original Gompertz equation depicts the time vs. death rate relation in a single population and is formulated as follows

$$Y(t) = \gamma \cdot \exp[-\alpha \cdot \exp(-\beta t)] \quad (\alpha > 1, 0 < \beta < 1, \gamma > 0) \quad (1)$$

where  $Y(t)$  and  $t$  denote death rate and year elapsed (1, 2, ...,  $n$ ), respectively, and  $\alpha$ ,  $\beta$ , and  $\gamma$  are the parameters that individually characterize Eq. 1. In the original Gompertz equation, the residual population after infinite time has elapsed (lower asymptote) is assumed to be zero, but resting muscle force (preload) is not. To meet the finite resting force, the upper asymptote  $\gamma_0$ , which reflects total load, was newly introduced. Thus the equation that yields instantaneous force  $F(t)$  during the isometric relaxation phase is formulated as follows

$$F(t) = \gamma_0 - Y(t) \quad (2)$$

Derivation for estimation of the regression equation is described in detail in APPENDIX A. Briefly,  $\gamma_0$  was determined through iteration in which  $\gamma_0$  was set at maximum  $F(t)$  at first and then increased stepwise by 0.5 mN/mm<sup>2</sup> until the minimum sum of square error was obtained. Differentiating Eq. 2 (see Eq. B3 in APPENDIX B)

$$\begin{aligned} dF(t)/dt &= -dY(t)/dt \\ &= -\alpha \cdot \beta \cdot \exp(-\beta t) \cdot Y(t) \\ &= -\alpha \cdot \beta \cdot \exp(-\beta t) \cdot [\gamma_0 - F(t)] \end{aligned} \quad (3)$$

yields the rate of force decay during the isometric relaxation phase. According to Eq. 3,  $dF(t)/dt$  is a product of the exponential term and the instantaneous force difference from its peak. Because  $\gamma_0 - F(t)$  is zero at the beginning of isometric relaxation,  $dF(t)/dt$  is zero at that instant. After  $dF(t)/dt$  attains its negative peak,  $dF(t)/dt$  approaches zero again at the end of the isometric relaxation phase, because  $\exp(-\beta t)$  asymptotically approaches zero. Equation 3 also suggests that at the terminal portion of isometric relaxation where  $\gamma_0 - F(t)$  can be regarded to be constant,  $dF(t)/dt$  should gradually approach the exponential function. The computer program that calculates values of  $\alpha$ ,  $\beta$ ,  $\gamma$ , and  $\gamma_0$  was developed in Turbo PASCAL 6.0 employing a numeric coprocessor, and graphic output was displayed on an X-Y plotter. To eliminate the data in the isotonic phase, data points of the top 2.5% and bottom 2.5% of developed force were discarded. The  $\tau_\beta$  was defined as

$$\tau_\beta = \text{sampling interval}/\beta \quad (4)$$

and has a dimension of the sampling interval.

Figure 2 shows computer-generated, double-exponential curves in the time domain. Bold lines show curves at  $\alpha = 5$  while (from left)  $\beta$  decreased from 0.2 to 0.05 stepwise by 0.025; fine lines show curves at  $\beta = 0.1$  while (from left)  $\alpha$  increased from 10 to 50 stepwise by 5. In Fig. 2, one may intuitively anticipate that  $\beta$  predominantly governs the slope of  $F(t)$ . On the other hand,  $\alpha$  reflects phasic delay of  $F(t)$  but does not affect its downward slope.

Figure 3 shows a phase-plane diagram, i.e., the  $F(t)$  vs.  $dF(t)/dt$  relation of the double-exponential function. Fine lines denote the relation at  $\gamma = 10$ , while  $\beta$  increased from 0.05 to 0.2 stepwise by 0.025; bold lines denote relation at  $\beta = 0.1$ , while (from left)  $\gamma$  increased from 10 to 20 stepwise by 2.5. Changes in  $\alpha$  do not alter Fig. 3. This is also supported by the fact that Eq. B5 (see APPENDIX B), which depicts the  $F(t)$  vs.  $dF(t)/dt$  relation, does not include  $\alpha$ . Maximal downslope of the curve is derived (Eq. B9) as follows

$$dF(t)/dt_{\max} = -\beta\gamma/e \quad (5)$$

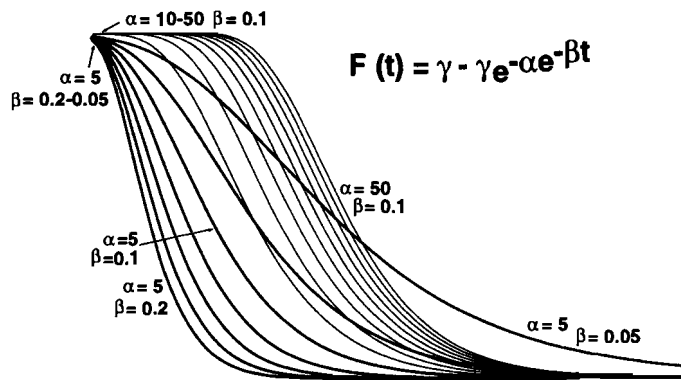


Fig. 2. Computer-generated Gompertz curves. Gompertz equation is defined under conditions of  $\alpha > 1$ ,  $0 < \beta < 1$ ,  $\gamma > 0$ . Upper asymptote ( $\gamma_0$ ) is arbitrarily set equal to  $\gamma$ , and lower asymptote ( $\gamma_0 - \gamma$ ) is set to zero. Bold lines, effects of changes in  $\beta$  ( $\alpha$  is held constant at 5); fine lines, effects of changes in  $\alpha$  ( $\beta$  is kept at 0.1).

and is also independent of  $\alpha$ . Figure 3 also shows that the terminal limiting slope of the  $F(t)$  vs.  $dF(t)/dt$  trajectory [not the ratio of  $F(t)$  to  $dF(t)/dt$ , because the terminal point is not the origin] is uniquely determined by  $\beta$  alone, irrespective of  $\gamma$  (Eqs. B6 and B7).

#### Experimental Protocols

After 10–15 min of stabilization, we started muscle stimulation at a fixed rate of 60/min (cycle length 1,000 ms). The muscle was made to contract isometrically at first (the force generated by the torque generator was set so high that the lever never left the mechanical stopper) at various initial muscle lengths. Muscle force was normalized in terms of stress ( $\text{mN}/\text{mm}^2$ ), i.e., force divided by the cross-sectional area, under the assumption that the papillary muscle shape is cylindrical. During fully isometric twitches, the effect of changes in muscle length (preload) on  $\alpha$  and  $\tau_\beta$  was examined. Then the muscle was subjected to physiologically sequenced contraction under conditions of various preloads (resting muscle length), various total loads (level of isotonic load), and hence various extents of muscle shortening.

To examine the effects of inotropic drugs, global ischemia, and reperfusion on the current indexes of relaxation, muscle contraction was made fully isometric again.  $\text{CaCl}_2$  (0.5 mg of 2%  $\text{CaCl}_2$ , 25  $\mu\text{l}$ ) or isoproterenol (0.025  $\mu\text{g}$  of 0.0001% isoproterenol, 25  $\mu\text{l}$ ) was added to the perfusion blood to

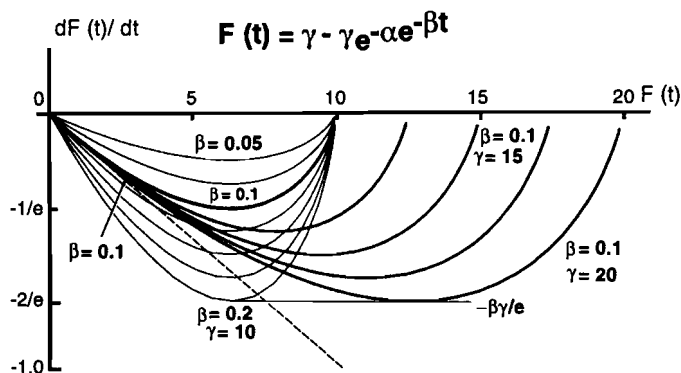


Fig. 3. Phase-plane diagram of Gompertz curve [ $F(t)$  vs.  $dF(t)/dt$  relation]. Changes in  $\alpha$  have no effect on phase-plane diagram, even though they produce phasic delay in time course of force decay (Fig. 2). Dashed line, tangent line for bold lines of  $\beta = 0.1$  at terminal point (terminal slope =  $-\beta$ ). Peak value of  $-dF(t)/dt$  is defined as  $-\beta\gamma/e$  and is  $-2/e$  when  $\beta = 0.2$  and  $\gamma = 10$  or  $\beta = 0.1$  and  $\gamma = 20$ .

enhance the myocardial contractility. The effects of global ischemia and subsequent reperfusion on  $\alpha$ ,  $\tau_\beta$ , and  $\tau$  were evaluated in isometric twitches around the end stage of each experiment. For the conventional exponential curve fitting, the data points were scanned for the steepest downward slope, and the data points between peak negative  $dF(t)/dt$  and those 2.5% (of developed force) above the resting force were acquired. Calculation of the regression equation between time and the logarithm of developed force with variable lower asymptote was repeated, increasing the lower asymptote stepwise by 0.5  $\text{mN}/\text{mm}^2$ , until the best correlation coefficient was obtained.

#### Statistical Analysis

In the physiologically sequenced isometric relaxation, regression analyses on the preload vs.  $\tau_\beta$  relation and on the preload vs.  $\tau$  relation were conducted within an individual muscle. To test the null hypothesis that the individual slope equals zero, Student's  $t$ -test was performed. Regression analyses on the total load vs.  $\tau_\beta$  relation and on the total load vs.  $\tau$  relation were conducted employing the same procedure. In isometric twitches, differences in values of  $\tau_\beta$  and  $\tau$  among interventions were tested employing analysis of variance (ANOVA) with Bonferroni's multiple comparison in compliance with the recommendation by Wallenstein et al. (17). All statistical analyses were conducted using SAS version 6.04 (SAS Institute, Cary, NC).

#### RESULTS

Table 1 shows baseline features of the papillary muscles and representative double-exponential regression equations and monoexponential regression equations during the physiologically sequenced isometric relaxation. Both correlation coefficients were  $> 0.995$ , and the double-exponential curve fitting showed slightly higher correlation coefficients than those of monoexponential regression. A muscle that has a higher value of  $\tau_\beta$  has a higher value of  $\tau$  (in Table 1, values of  $\beta$  and  $B$  are shown instead of  $\tau_\beta$  and  $\tau$ , respectively). Values of  $\tau_\beta$  were stable and reproducible as long as the myocardial state that regulates relaxation was kept unchanged; e.g.,  $\tau_\beta$  in 45 arbitrarily chosen fully isometric twitches under conditions of widely varied preload ( $2.4$ – $13.2$   $\text{mN}/\text{mm}^2$ ) in muscle 6 (developed stress  $15.7$ – $67.0$   $\text{mN}/\text{mm}^2$ ) was  $76.0 \pm 0.57$  (SD) ms. The correlation coefficient on  $\tau_\beta$  was  $0.99984 \pm 0.00006$  (SD). The  $\tau$  derived from monoexponential curve fitting was  $106.5 \pm 7.9$  ms, and the correlation coefficient was  $0.99907 \pm 0.00097$ . In the physiologically sequenced contraction, 56 isometric twitches of muscle 6 were evaluated in the same manner under various preloads ( $3.64$ – $16.8$   $\text{mN}/\text{mm}^2$ ) and total loads ( $19.3$ – $50.0$   $\text{mN}/\text{mm}^2$ ). The  $\tau_\beta$  was  $73.7 \pm 2.55$  ms, and the correlation coefficient on  $\tau_\beta$  was  $0.99986 \pm 0.00004$ . The  $\tau$  derived through the conventional exponential curve fitting on the same data was  $88.9 \pm 11.1$  ms, and the correlation coefficient was  $0.99789 \pm 0.00159$ .

On the other hand, efficacy of  $\alpha$  in evaluating relaxation characteristics seemed to highly depend on how the onset of the isometric relaxation phase was identified. The  $\alpha$  in the double-exponential curve fitting was  $3.45 \pm 0.32$  (SD) ( $n = 45$ ) on the isometric twitch and  $4.37 \pm 0.33$  ( $n = 56$ ) on the physiologically sequenced

Table 1. Basic features of papillary muscles during control state

Muscle No.	$L_{\max}$ , mm	CSA, mm <sup>2</sup>	Max Stress, mN/mm <sup>2</sup>	Max $\Delta L/L_{\max}$	Regression Equation $F(t) = \gamma_0 - \gamma \cdot \exp[-\alpha \cdot \exp(-\beta t)]$ $F(t) = A \cdot \exp(-B \cdot t)$	Correlation Coeff
1	10.4	9.35	51.4	0.135	$F(t) = 25.0 - 20.3 \cdot \exp[-3.1 \cdot \exp(-0.147t)]$ $F(t) = 14.6 \cdot \exp(-0.104t)$	0.99990 0.99964
2	8.4	4.58	62.2	0.139	$F(t) = 54.0 - 49.3 \cdot \exp[-4.8 \cdot \exp(-0.151t)]$ $F(t) = 32.1 \cdot \exp(-0.143t)$	0.99987 0.99946
3	10.0	6.04	78.1	0.243	$F(t) = 41.9 - 40.4 \cdot \exp[-3.1 \cdot \exp(-0.117t)]$ $F(t) = 30.5 \cdot \exp(-0.081t)$	0.99984 0.99952
4	7.8	5.02	62.4	0.170	$F(t) = 66.6 - 58.9 \cdot \exp[-3.1 \cdot \exp(-0.083t)]$ $F(t) = 49.5 \cdot \exp(-0.050t)$	0.99980 0.99891
5	8.0	6.66	75.3	0.132	$F(t) = 38.6 - 27.9 \cdot \exp[-4.3 \cdot \exp(-0.137t)]$ $F(t) = 18.2 \cdot \exp(-0.113t)$	0.99992 0.99875
6	9.0	5.85	72.6	0.169	$F(t) = 67.6 - 56.1 \cdot \exp[-3.8 \cdot \exp(-0.130t)]$ $F(t) = 42.6 \cdot \exp(-0.089t)$	0.99965 0.99957
7	11.3	6.79	58.1	0.123	$F(t) = 50.7 - 46.2 \cdot \exp[-3.2 \cdot \exp(-0.130t)]$ $F(t) = 32.5 \cdot \exp(-0.094t)$	0.99987 0.99971
8	10.0	7.59	45.9	0.111	$F(t) = 28.6 - 26.7 \cdot \exp[-3.1 \cdot \exp(-0.118t)]$ $F(t) = 17.8 \cdot \exp(-0.076t)$	0.99973 0.99972
Mean $\pm$ SD	$9.36 \pm 1.25$	$6.51 \pm 1.56$	$63.25 \pm 11.48$	$0.153 \pm 0.042$	$F(t) = 46.6 \pm 16.0 - 40.7 \pm 14.4 \cdot \exp[-3.6 \pm 0.67 \cdot \exp(-0.127 \pm 0.021t)]$ $F(t) = 29.7 \pm 12.4 \cdot \exp(-0.094 \pm 0.028t)$	$0.99982 \pm 0.000094$ $0.99941 \pm 0.00037$

CSA, cross-sectional area;  $L_{\max}$ , resting muscle length at which developed force is maximum; Max stress, maximum force divided by CSA in an isometric twitch at  $L_{\max}$ . Max stress was observed during fully isometric contractions. Max  $\Delta L/L_{\max}$  was observed during afterloaded isotonic contractions with light afterload.

relaxation. According to Eq. B5, the  $F(t)$  vs.  $dF(t)/dt$  relation of the double-exponential function is independent of  $\alpha$ . In fully isometric twitches,  $\alpha$  readily represents phasic delay of the relaxation onset as long as the double-exponential curve fitting starts from its peak force. In the physiologically sequenced relaxation, identification of the isometric relaxation onset is difficult because of the smooth transition in force from the isotonic phase to the convexly decaying phase. As displayed in Fig. 2, changes in  $\alpha$  mainly affect the initial part of force decay. The uncertainty in identification of the isometric relaxation onset will lead to noticeable error in the estimation of  $\alpha$ . In contrast,  $\beta$  (expressed in terms of  $\tau_\beta$  in the present study) showed a robustness against variation in the region of data acquisition and was sensitive to changes in the myocardial lusitropic state. Hence, in the current study, evaluation of changes in  $\alpha$  was circumscribed within fully isometric twitches.

#### Physiologically Sequenced Isometric Relaxation

**Relation between preload and  $\tau_\beta$ .** Figure 4 shows four representative traces of the physiologically sequenced relaxation under conditions of constant isotonic load and varying preload. The double-exponential curve fitting of the isometric force decay showed high correlation coefficients in all traces ( $R \geq 0.9998$ ). In Fig. 4, *left*, four bold lines, which overlap as if they are identical, denote muscle stress traces. The four equations in Fig. 4, *bottom*, denote their double-exponential regression equations, and the four fine lines in Fig. 4, *left* (illegible because of overlapping), show their regression lines generated from the corresponding regression equations. In Fig. 4, the traces are aligned by the time of the muscle length clamp to show the overlapped time course of force decline at various preloads. The  $\alpha$  remained unchanged

despite substantial variations in the duration of the isotonic shortening phase. Values of  $\tau$  obtained through the conventional monoexponential curve fitting were (from *top*) 0.112, 0.110, 0.090, and 0.104 s, respectively (not shown). Figure 4, *right*, is the phase-plane diagram of the four contractions, which displays the invariable  $F(t)$  vs.  $dF(t)/dt$  relation in *quadrant IV* (the isometric relaxation phase). The fine line in *quadrant IV* (illegible because of overlapping) denotes the phase-plane diagram of the regression Eq. 1, which is shown in Fig. 4, *bottom*. For legibility, phase-plane trajectories of the regression equations are omitted thereafter. Regression analysis on the preload vs.  $\tau_\beta$  relation was performed on muscles 2–7 and summarized in Fig. 5. The null hypothesis that the slope of the individual muscle equals zero was rejected in muscle 4 ( $P = 0.003$ ) and muscle 6 ( $P = 0.004$ ). However, the slope constants of  $\tau_\beta$  were negligible (0.0002 and 0.00028 s  $\cdot$  mN<sup>-1</sup>  $\cdot$  mm<sup>-2</sup>, respectively) compared with their corresponding intercepts (0.13 and 0.079 s, respectively). The regression analysis of the relation between preload and monoexponential time constant  $\tau$  is also shown in Table 2. The mean slope of  $\tau$  was  $\sim 2.3$  times greater than that of  $\tau_\beta$ .

**Relation between total load and  $\tau_\beta$ .** The time courses of tension fall at five levels of total load in the physiologically sequenced relaxation are shown in Fig. 6, *left*. Values of  $\alpha$  and  $\tau_\beta$  of the double-exponential regression equation were practically invariable despite wide variations in total load, extent of muscle shortening, and end-systolic fiber length. In the physiologically sequenced relaxation, the time course of force decay was convex at first and then concave. This is true even at a very low level of total load (e.g., Fig. 6, *trace 5*). Because premature muscle length clamp produces a force redevelopment above the isotonic level and delayed muscle

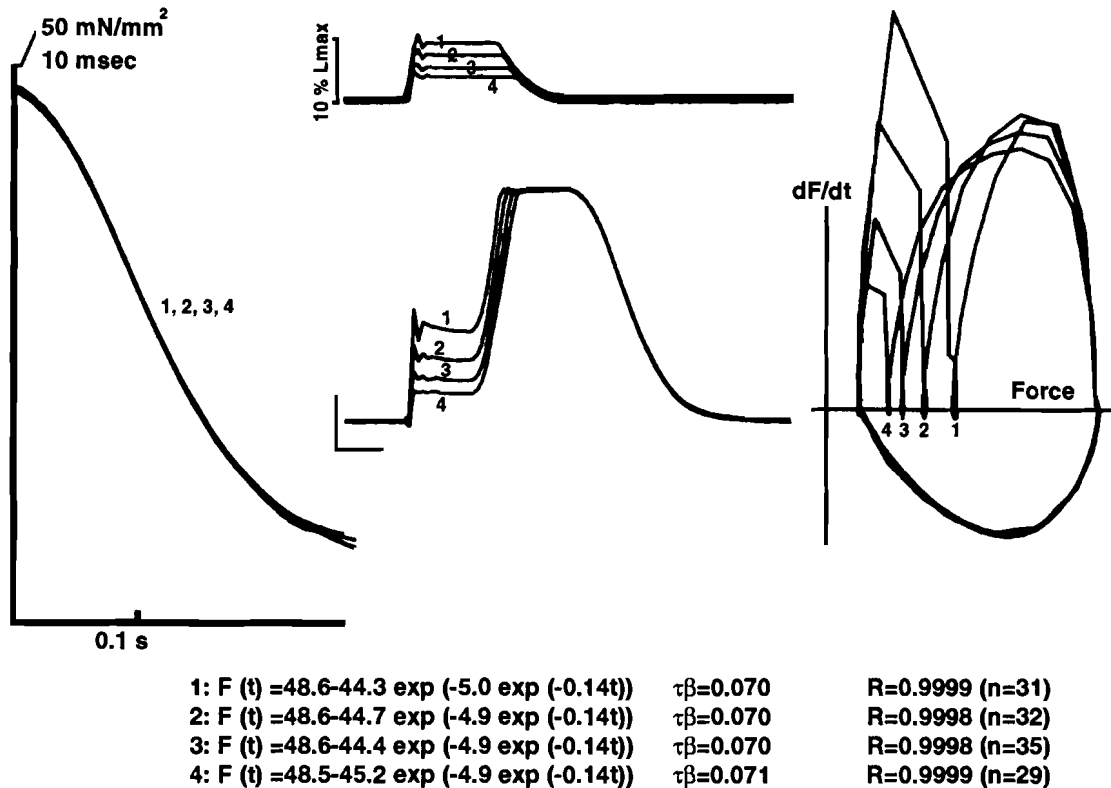


Fig. 4. Four representative traces (1-4) of physiologically sequenced isometric relaxation at various preloads. *Middle*: muscle length and force traces are aligned by end-systolic point (instant that muscle stress begins to fall) to emphasize an identical time course of force decline. A small right angle shows 10 mN/mm<sup>2</sup> force scale (vertical bar) and 0.1-s time scale (horizontal bar). *Left*: 4 stress traces and their regression lines are superimposed. *Right*: phase-plane diagram of 4 twitches. 1-4, Correspondence between trace and regression equation at *bottom*. Fine line at *right*, phase-plane diagram of regression Eq. 1 at *bottom*. Unit of  $\tau\beta$  is s.

length clamp leads to discontinuity in force trace (sudden transition in force from the isotonic level to rectilinear or concave force decline), the timing of the muscle length clamp was carefully adjusted for the smooth transition of force in the present study. At the end of muscle shortening (the instant of the shortest muscle length), the muscle motion could be regarded to be

quasi static. The muscle length clamp at that "dead point" should never produce an abrupt change in muscle force or muscle length.

Figure 6, *right*, shows the phase-plane diagram of five representative twitches. Contrary to the description by Sys and Brutsaert (14), the phase-plane trajectory at a lower isotonic load did not trace that of a higher isotonic load or that of a fully isometric twitch on the way to its terminal point. As shown in Fig. 6, *right*, there was a significant leftward shift of the phase-plane trajectory in *quadrant IV*, when the isotonic load was reduced, indicating substantial changes in the force vs. rate of force relation. However, the terminal slope of the phase-plane trajectories (see APPENDIX B) seems invariable. Figure 7 shows the relation between total load (isotonic load) and  $\tau\beta$  in five muscles. Regression analysis between total load and  $\tau\beta$  and that between total load and  $\tau$  on the individual muscle are summarized in Table 3. In the double-exponential curve fitting, the slopes of regression equations could not be regarded to be zero, except for *muscle 2*; however, all slope values were negligible [ $-0.00014 \pm 0.00019$  (SD)  $s \cdot mN^{-1} \cdot mm^{-2}$ ] compared with their corresponding intercepts ( $0.0762 \pm 0.019$  s). The mean regression slope of the conventional exponential curve fitting ( $-0.00034 \pm 0.00011$   $s \cdot mN^{-1} \cdot mm^{-2}$ ) is 2.4 times greater than that of the present method. Because Bartlett's test rejected the null hypothesis of

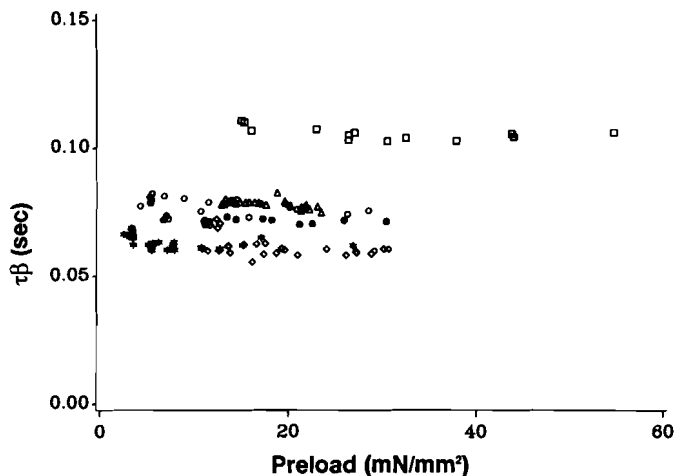


Fig. 5. Relation between preload and  $\tau\beta$  (muscles 2-7) in physiologically sequenced isometric relaxation. ●, Muscle 2; ○, muscle 3; □, muscle 4; △, muscle 5; ◇, muscle 6; \*, muscle 7.

Table 2. Preload vs.  $\tau_\beta$  and  $\tau$  relation in physiologically sequenced contraction

Muscle No.	Regression Equation $F(t) = A + B \cdot \tau_\beta$	$R^2$	$P(H_0: \text{slope} = 0)$
2	$F(t) = 0.066 - 0.000001 \cdot \tau_\beta$	0.004 ( $n = 22$ )	0.765
3	$F(t) = 0.089 - 0.000001 \cdot \tau_\beta$	0.000 ( $n = 22$ )	0.978
4	$F(t) = 0.130 - 0.000200 \cdot \tau_\beta$	0.286 ( $n = 27$ )	0.003
5	$F(t) = 0.076 - 0.000134 \cdot \tau_\beta$	0.049 ( $n = 36$ )	0.185
6	$F(t) = 0.079 - 0.000287 \cdot \tau_\beta$	0.176 ( $n = 45$ )	0.004
7	$F(t) = 0.076 + 0.000017 \cdot \tau_\beta$	0.002 ( $n = 24$ )	0.784
Mean $\pm$ SD $F(t) = 0.0860 \pm 0.023 - 0.00010 \pm 0.00013 \cdot \tau_\beta$ ( $n = 6$ )			

Muscle No.	Regression Equation $F(t) = A + B \cdot \tau$	$R^2$	$P(H_0: \text{slope} = 0)$
2	$F(t) = 0.074 - 0.000169 \cdot \tau$	0.218 ( $n = 22$ )	0.025
3	$F(t) = 0.121 - 0.000402 \cdot \tau$	0.692 ( $n = 22$ )	0.0001
4	$F(t) = 0.233 - 0.000130 \cdot \tau$	0.006 ( $n = 27$ )	0.708
5	$F(t) = 0.096 - 0.000453 \cdot \tau$	0.131 ( $n = 36$ )	0.028
6	$F(t) = 0.116 - 0.000205 \cdot \tau$	0.052 ( $n = 45$ )	0.128
7	$F(t) = 0.120 - 0.000017 \cdot \tau$	0.001 ( $n = 24$ )	0.891
Mean $\pm$ SD $F(t) = 0.1267 \pm 0.055 - 0.00023 \pm 0.00017 \cdot \tau$ ( $n = 6$ )			

homoscedasticity of regression residuals in all combinations involving  $\tau_\beta$  and  $\tau$  ( $P < 0.01$ ), analysis of covariance was abandoned.

#### Fully Isometric Contraction and Relaxation (Isometric Twitch)

**Effect of changes in muscle length (preload) on  $\tau_\beta$ .** The effects of muscle length (preload) alteration on  $\alpha$  and  $\tau_\beta$  were evaluated in the fully isometric twitch. Contrary to the physiologically sequenced relaxation in which the isotonic phase seamlessly enters the isometric relaxation phase, the onset of isometric relaxation in the fully isometric twitch was easily identified as the time of peak force. Data processing was the same as that of the physiologically sequenced contraction (values in the middle 95% of force were used for analysis). Under conditions of widely varied initial muscle length and peak muscle stress,  $\tau_\beta$  remained practically invariable (Fig. 8). The relation between preload and  $\tau_\beta$  is plotted in Fig. 9 (data in *muscle 2* were eliminated for legibility). The zero slope hypothesis of the preload vs.  $\tau_\beta$  relation was rejected in *muscles 2* and *5*; however, these slopes were as small as one-tenth of those of  $\tau$ . In Table 4, the relations between preload and  $\tau_\beta$  and between preload and  $\tau$  are summarized. No significant change in  $\alpha$  was

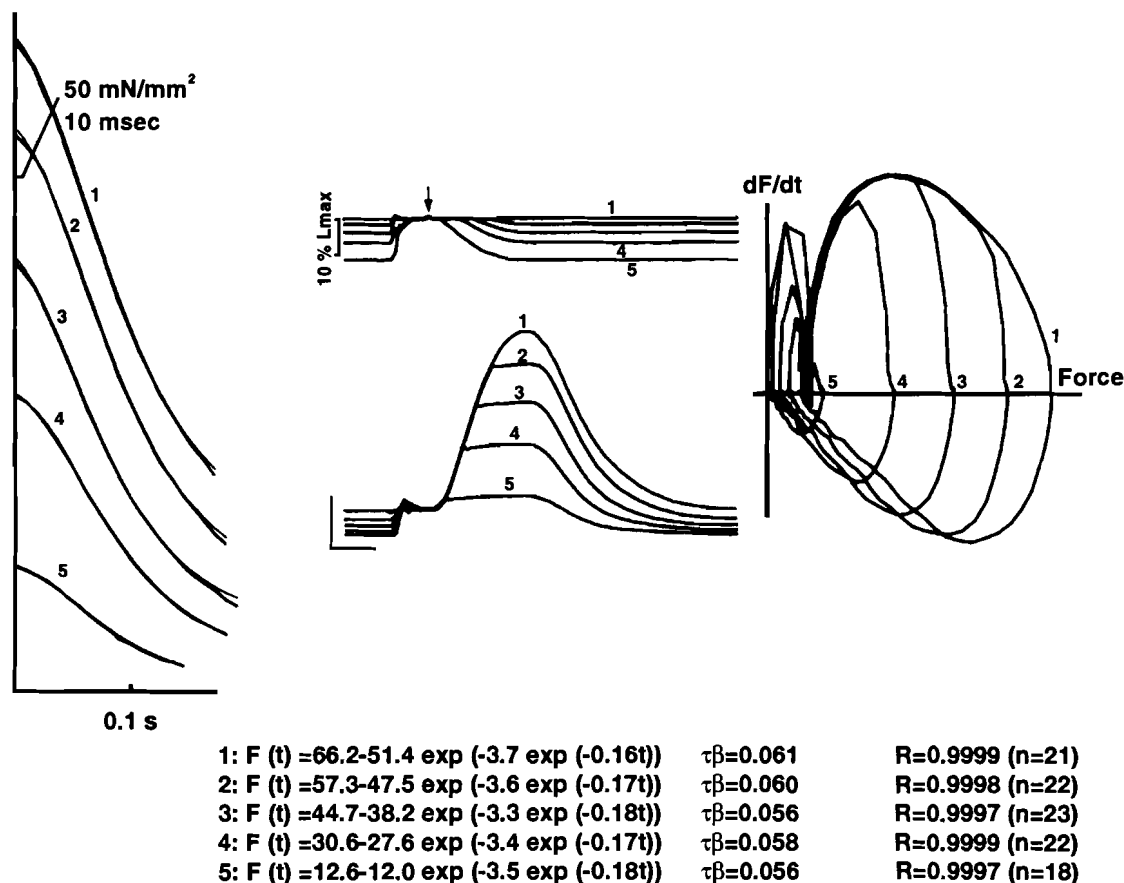


Fig. 6. Five representative traces (1–5) of physiologically sequenced isometric relaxation at various total loads. See legend to Fig. 4 for details. Arrow on muscle length trace in *middle* denotes time of muscle stimulation. Isometric force declines in a reversed S shape, even under lowest level of isotonic load. Decrement in isotonic load shifts terminal portion of phase-plane trajectory leftward.

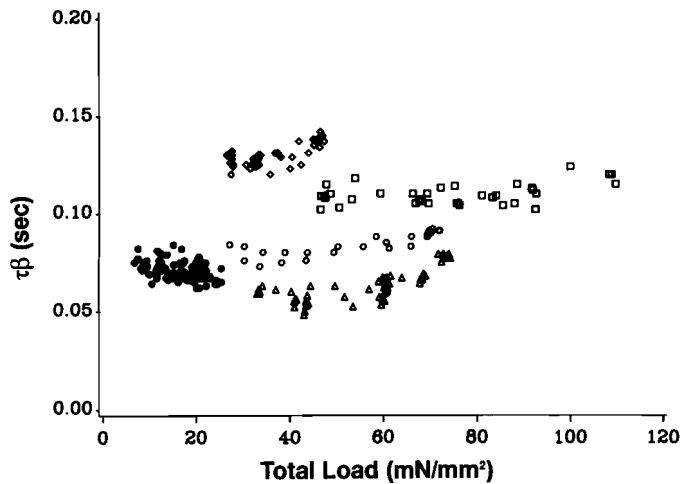


Fig. 7. Relation between total load and  $\tau_\beta$ . Data for muscles 2, 5, and 7 are omitted for legibility. ●, Muscle 1; ○, muscle 3; □, muscle 4; △, muscle 6; ◇, muscle 8.

detected despite a wide variation in preload and peak stress in the fully isometric twitch.

*Effect of isoproterenol,  $\text{CaCl}_2$ , global ischemia, and subsequent reperfusion on  $\tau_\beta$  in the fully isometric twitch.*  $\text{CaCl}_2$  and isoproterenol produce a marked increase in peak force and an enhanced rate of force development. In both interventions,  $\tau_\beta$  substantially decreased (Table 5), but  $\alpha$  was practically unchanged (Table 6). To assess the effects of global ischemia and subsequent reperfusion on  $\tau_\beta$  and  $\tau$ , the line that supplied arterial blood for the specimen muscle was transiently occluded for 90 s. During global ischemia, peak stress fell sharply and the duration of muscle force maintenance was markedly curtailed (Fig. 10, trace 2). Concomitantly,  $\tau_\beta$  was substantially reduced in all muscles during ischemia. The  $\tau$  obtained through the conventional method decreased in muscles 3, 5, and 7; however, in muscles 1, 2, and 6,  $\tau$  showed no significant

change ( $P < 0.01$ ; Table 5). After resumption of blood perfusion,  $\tau_\beta$  and  $\tau$  increased in association with retardation of force decline, as previously reported by Bing et al. (1). An ANOVA test on  $\tau_\beta$  with Bonferroni's multiple comparison using proc GLM in SAS detected a significant difference among interventions ( $P < 0.01$ ), except for the combination of  $\text{CaCl}_2$  and isoproterenol (Fig. 11). In the conventional exponential curve fitting, the behavior of  $\tau$  resembled that of  $\tau_\beta$ .

*Effect of isoproterenol,  $\text{CaCl}_2$ , ischemia, and reperfusion on  $\alpha$  in the fully isometric twitch.* Global ischemia significantly reduced  $\alpha$ , and reperfusion increased it. An ANOVA test with Bonferroni's multiple comparison detected a significant difference ( $P < 0.01$ ) among mean values of  $\alpha$  involving ischemia and reperfusion. No significant difference in mean values of  $\alpha$  among the other combinations (control,  $\text{CaCl}_2$ , and isoproterenol) were detected ( $P < 0.01$ ). Changes in  $\alpha$  during these interventions are summarized in Fig. 12.

## DISCUSSION

The purpose of the present study is to propose new reproducible load-independent indexes of isometric myocardial relaxation that are feasible throughout the fully isometric twitch and the physiologically sequenced isometric relaxation. In the conventional afterloaded isotonic contraction, the onset of the isometric relaxation is characterized by a sudden interruption of muscle re-lengthening. At that moment, the isotonic lever suddenly ceases its upward motion, colliding against a mechanical stopper. The papillary muscle continues to lengthen owing to its own momentum, and a slacking (or a sudden decrease in tension) in the mechanical linkage between the muscle and a force transducer occurs. The steep downward deflection in muscle force at the onset of isometric relaxation in the conventional afterloaded contraction, which was named "an abrupt fall in tension" by Parmley and Sonnenblick (11), must be ascribed to this slacking or its reflection wave. In the working ventricle with normal aortic valve function in situ, such a mechanical discontinuity never occurs. Strictly speaking, aortic valve closure inevitably accompanies cusp motion toward the ventricle in association with minimal regurgitation just before complete closure. Hence the onset of a genuine isovolumic relaxation phase should commence several milliseconds after the moment of minimum ventricular volume. An upward notch in high-fidelity aortic pressure recording and a corresponding reciprocal downward incisor in the left ventricular pressure trace just after the aortic valve closure should be attributed to the sudden interruption of regurgitating flow by the completion of valve closure (12). From the conceptual point of view, nevertheless, the muscle length clamp at the shortest muscle length without mechanical discontinuity is the most pertinent mechanical model of myocardial relaxation in the ventricular wall. For this reason, the isometric relaxation at the initial muscle length in the conventional afterloaded isotonic contraction, in which a simple monoexponential

Table 3. Total load vs.  $\tau_\beta$  and  $\tau$  relation in physiologically sequenced contraction

Muscle No.	Regression Equation $F(t) = A + B \cdot \tau_\beta$	$R^2$	$P(H_0: \text{slope} = 0)$
2	$F(t) = 0.070 - 0.000003 \cdot \tau_\beta$	0.015 ( $n = 31$ )	0.512
3	$F(t) = 0.074 + 0.000022 \cdot \tau_\beta$	0.736 ( $n = 28$ )	0.0001
4	$F(t) = 0.111 + 0.000018 \cdot \tau_\beta$	0.641 ( $n = 38$ )	0.0001
5	$F(t) = 0.081 - 0.000016 \cdot \tau_\beta$	0.392 ( $n = 24$ )	0.0008
6	$F(t) = 0.055 + 0.000030 \cdot \tau_\beta$	0.739 ( $n = 64$ )	0.0001
7	$F(t) = 0.066 + 0.000031 \cdot \tau_\beta$	0.461 ( $n = 41$ )	0.0001
Mean $\pm$ SD	$F(t) = 0.0762 \pm 0.019 - 0.00014 \pm 0.00019 \cdot \tau_\beta$ ( $n = 6$ )		
Muscle No.	Regression Equation $F(t) = A + B \cdot \tau$	$R^2$	$P(H_0: \text{slope} = 0)$
2	$F(t) = 0.067 + 0.00014 \cdot \tau$	0.114 ( $n = 31$ )	0.059
3	$F(t) = 0.112 + 0.00040 \cdot \tau$	0.765 ( $n = 28$ )	0.0001
4	$F(t) = 0.187 + 0.00045 \cdot \tau$	0.221 ( $n = 38$ )	0.003
5	$F(t) = 0.074 + 0.00039 \cdot \tau$	0.090 ( $n = 24$ )	0.145
6	$F(t) = 0.086 + 0.00038 \cdot \tau$	0.418 ( $n = 64$ )	0.0001
7	$F(t) = 0.099 + 0.00030 \cdot \tau$	0.213 ( $n = 41$ )	0.0003
Mean $\pm$ SD	$F(t) = 0.104 \pm 0.044 - 0.00034 \pm 0.00011 \cdot \tau$ ( $n = 6$ )		

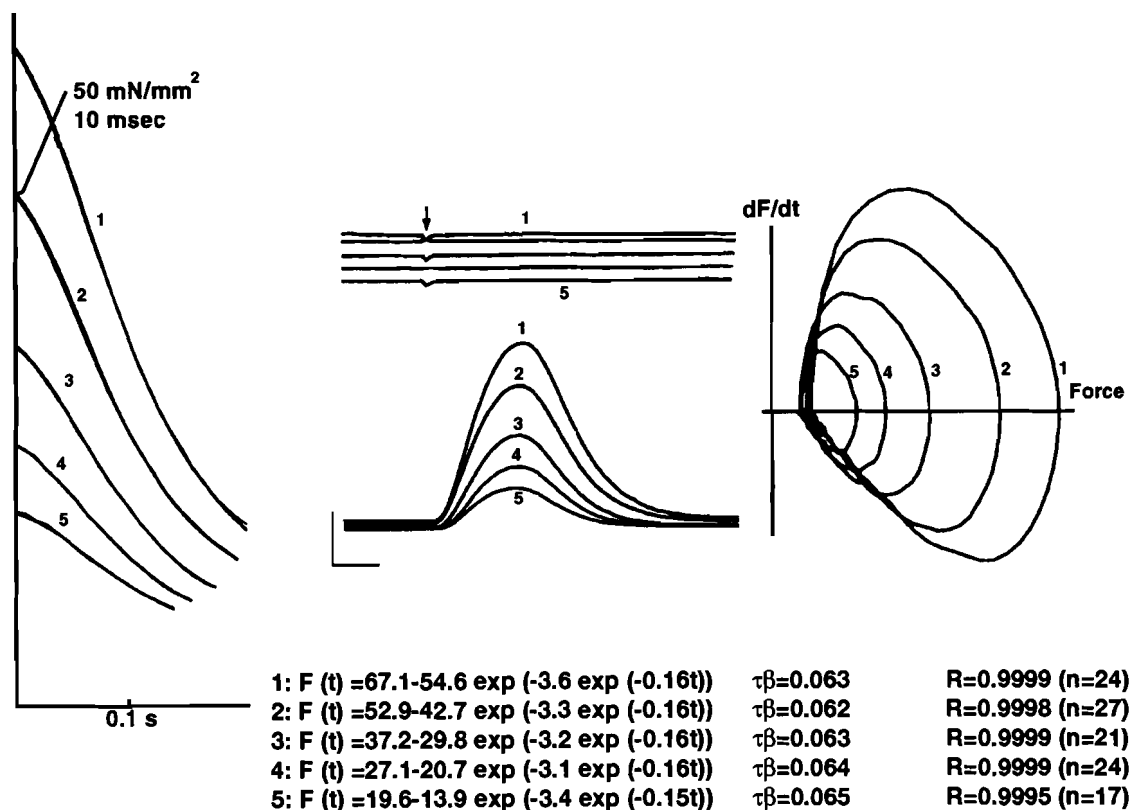


Fig. 8. Five representative fully isometric twitches (1–5) at various preloads. See legends to Figs. 4 and 6 for details.

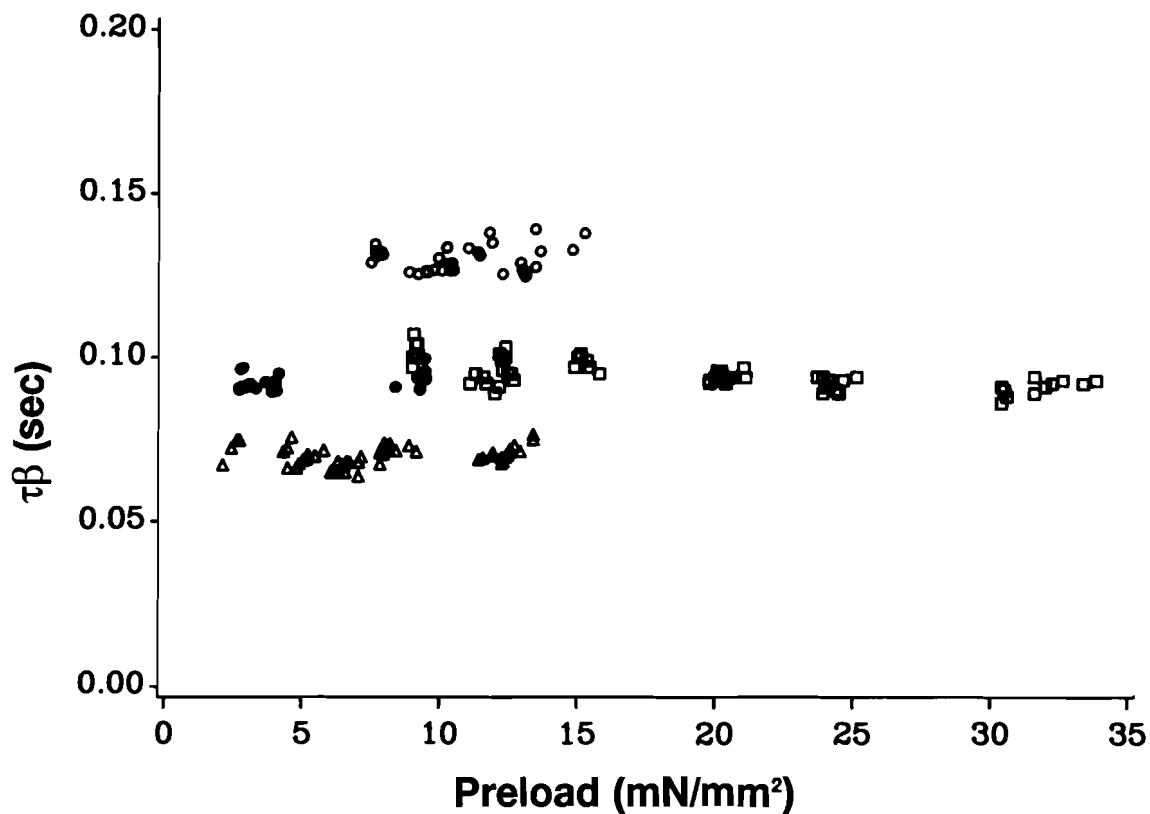


Fig. 9. Relation between preload and  $\tau\beta$  in fully isometric twitches. Data for *muscle 2* are omitted for legibility. ●, *Muscle 1*; ○, *muscle 4*; □, *muscle 5*; △, *muscle 6*.



Table 4. *Preload vs.  $\tau_\beta$  and  $\tau$  relation in isometric twitch*

Muscle No.	Regression Equation $F(t) = A + B \cdot \tau_\beta$	$R^2$	$P(H_0: \text{slope} = 0)$
1	$F(t) = 0.091 + 0.00023 \cdot \tau_\beta$	0.659 ( $n = 23$ )	0.226
2	$F(t) = 0.082 - 0.00069 \cdot \tau_\beta$	0.106 ( $n = 38$ )	0.043
4	$F(t) = 0.127 + 0.00025 \cdot \tau_\beta$	0.182 ( $n = 34$ )	0.440
5	$F(t) = 0.102 - 0.00038 \cdot \tau_\beta$	0.455 ( $n = 66$ )	0.0001
6	$F(t) = 0.069 - 0.00018 \cdot \tau_\beta$	0.039 ( $n = 54$ )	0.148
Mean $\pm$ SD	$F(t) = 0.0942 \pm 0.0220 - 0.000154 \pm 0.00040 \cdot \tau_\beta$ ( $n = 5$ )		

Muscle No.	Regression Equation $F(t) = A + B \cdot \tau$	$R^2$	$P(H_0: \text{slope} = 0)$
1	$F(t) = 0.107 - 0.01437 \cdot \tau$	0.775 ( $n = 23$ )	0.0001
2	$F(t) = 0.073 + 0.00003 \cdot \tau$	0.0005 ( $n = 38$ )	0.934
4	$F(t) = 0.160 + 0.00581 \cdot \tau$	0.277 ( $n = 34$ )	0.0008
5	$F(t) = 0.169 - 0.00208 \cdot \tau$	0.542 ( $n = 66$ )	0.0001
6	$F(t) = 0.089 + 0.00216 \cdot \tau$	0.682 ( $n = 54$ )	0.0001
Mean $\pm$ SD	$F(t) = 0.1196 \pm 0.043 - 0.00169 \pm 0.00766 \cdot \tau$ ( $n = 5$ )		

force decay was reported after the abrupt fall in tension (11), was excluded from our study.

The monoexponential curve fitting, which was originally advocated through the observation of the conventional afterloaded contraction (7, 11), has been applied to ejecting and nonejecting ventricles (4, 8, 18). According to Weiss and co-workers (18), the exponential time constant  $T$ , which is expected to have a linear relation to  $\tau$  of the current study, was independent of systolic stress and end-systolic fiber length and dependent on systolic fiber shortening.  $\text{CaCl}_2$  and ischemia resulted in no significant change in  $T$ , but norepinephrine shortened  $T$ , and recovery from ischemia prolonged  $T$ . A monoexponential curve fitting implicitly assumes a rectilinear relation between the instantaneous force and the rate of force decline. This is easily understood by the fact that the first derivative of an exponential equation with respect to time is an exponential function again. Hence, the exponential curve fitting is expected to provide a correction for the dependence of the rate of pressure fall on instantaneous ventricular pressure, as far as the pressure falls exponentially.

Recently, utilizing the phase-plane diagram (instantaneous force vs. rate of force decline relation), Sys and Brutsaert (14) proposed a method to evaluate isometric relaxation. They found that changes in contraction load affected the time of onset but not the time course of

force decline. In other words, muscle shortening advanced the onset of relaxation but did not affect the rate of relaxation. They concluded that the myocardial lusitropic state was predominantly characterized by the unique relation between muscle force and the rate of force decline in its terminal point (end of isometric relaxation). The relation between instantaneous muscle force and the rate of force decline of the double-exponential function is derived as *Eq. B5*, which does not include  $\alpha$ , and is displayed in Fig. 3. Apparently, the terminal slopes of the bold lines, of which  $\beta$  was held constant, seem to converge, and the terminal slope seems to be governed by  $\beta$  alone, irrespective of  $\gamma$ . In fact, it is proved that the limit value of the terminal slope in the phase-plane trajectory of the double-exponential curve yields  $-\beta$  (*Eqs. B6 and B7*). In this context, the current study is a justifiable extension of the conventional exponential curve fitting. It approves the proposal by Sys and Brutsaert that a quantitative measure of the rate of force decline could be obtained from the slope of the phase-plane trace in the origin, i.e., near the end of isometric relaxation, when developed force and rate of force decline tend toward zero. Sys and Brutsaert mentioned that this measure can be interpreted as a limit of the time constant of a piecewise exponential approach to force decline as developed force tends to zero, i.e., the time constant of terminal force decline. In *quadrant IV* of the phase-plane diagram,  $\tau$  directly relates to the reciprocal of the slope of the rectilinear monoexponential regression line, whereas  $\tau_\beta$  relates to the reciprocal of the terminal slope of the curvilinear double-exponential function. Thus the monoexponential time constant  $\tau$ , which is conventionally determined not near the end of relaxation but in the vicinity of its maximum slope, tended to be longer than  $\tau_\beta$ . Sys and Brutsaert also argued that at low afterload the peak rate of force decline at that length could be underestimated when force decline started at a force level lower than the force at the peak slope of force. At a lower isotonic load, according to Sys and Brutsaert, the isometric muscle force abruptly begins to decline, with nonzero slope succeeding the isotonic phase. Extending the point of view of Sys and Brutsaert, the level of isotonic load determines a phasic window position through which a part of isometric force decline in the fully isometric twitch appears.

Table 5. *Effect of  $\text{CaCl}_2$ , isoproterenol, global ischemia, and reperfusion on mean values of  $\tau_\beta$  and  $\tau$  in fully isometric twitch*

Muscle No.	Control		$\text{CaCl}_2$ (0.5 mg)		Isoproterenol (0.025 $\mu\text{g}$ )		Global Ischemia		Reperfusion	
	$\tau_\beta$	$\tau$	$\tau_\beta$	$\tau$	$\tau_\beta$	$\tau$	$\tau_\beta$	$\tau$	$\tau_\beta$	$\tau$
1	0.098 $\pm$ 0.012	0.121 $\pm$ 0.004					0.081 $\pm$ 0.002	0.122 $\pm$ 0.002	0.103 $\pm$ 0.001	0.128 $\pm$ 0.004
2	0.063 $\pm$ 0.001	0.069 $\pm$ 0.003	0.053 $\pm$ 0.001	0.065 $\pm$ 0.001	0.049 $\pm$ 0.001	0.059 $\pm$ 0.002	0.056 $\pm$ 0.001	0.070 $\pm$ 0.036	0.070 $\pm$ 0.001	0.081 $\pm$ 0.002
3	0.128 $\pm$ 0.001	0.189 $\pm$ 0.007	0.079 $\pm$ 0.001	0.113 $\pm$ 0.001	0.074 $\pm$ 0.001	0.103 $\pm$ 0.002	0.094 $\pm$ 0.007	0.125 $\pm$ 0.027	0.138 $\pm$ 0.004	0.188 $\pm$ 0.005
5	0.083 $\pm$ 0.002	0.096 $\pm$ 0.010			0.063 $\pm$ 0.002	0.075 $\pm$ 0.004	0.054 $\pm$ 0.004	0.084 $\pm$ 0.013	0.108 $\pm$ 0.001	0.160 $\pm$ 0.012
6	0.070 $\pm$ 0.001	0.100 $\pm$ 0.001	0.064 $\pm$ 0.001	0.094 $\pm$ 0.001	0.061 $\pm$ 0.002	0.088 $\pm$ 0.001	0.062 $\pm$ 0.002	0.099 $\pm$ 0.002	0.096 $\pm$ 0.001	0.131 $\pm$ 0.007
7	0.098 $\pm$ 0.003	0.145 $\pm$ 0.003	0.076 $\pm$ 0.001	0.111 $\pm$ 0.001	0.065 $\pm$ 0.001	0.086 $\pm$ 0.004	0.054 $\pm$ 0.001	0.090 $\pm$ 0.003	0.085 $\pm$ 0.002	0.083 $\pm$ 0.002

Values are means  $\pm$  SD in s.

0.098

Table 6. *Effect of  $\text{CaCl}_2$ , isoproterenol, global ischemia, and reperfusion on  $\alpha$  in fully isometric twitch*

Muscle No.	Control	$\text{CaCl}_2$ (0.5 mg)	Isoproterenol (0.025 $\mu\text{g}$ )	Global Ischemia	Reperfusion
1	4.35 $\pm$ 0.13			2.25 $\pm$ 0.06	4.35 $\pm$ 0.06
2	4.85 $\pm$ 0.35	4.75 $\pm$ 0.31	4.80 $\pm$ 0.25	3.25 $\pm$ 0.06	4.63 $\pm$ 0.10
3	2.80 $\pm$ 0.08	3.25 $\pm$ 0.06	3.25 $\pm$ 0.06	2.45 $\pm$ 0.17	3.83 $\pm$ 0.13
5	4.40 $\pm$ 0.14		3.85 $\pm$ 0.31	2.78 $\pm$ 0.10	3.83 $\pm$ 0.15
6	3.40 $\pm$ 0.12	3.35 $\pm$ 0.13	3.38 $\pm$ 0.05	2.73 $\pm$ 0.05	3.28 $\pm$ 0.17
7	3.23 $\pm$ 0.13	2.93 $\pm$ 0.05	3.65 $\pm$ 0.24	2.55 $\pm$ 0.13	4.38 $\pm$ 0.10

Values are means  $\pm$  SD.

From the technical point of view, there are several ways to keep the muscle at its shortest length during the isometric relaxation phase. The oldest method was reported by Jewell and Wilkie (7). The second, which we reported (15) and used in the current study, employs direct mechanical lock of the isotonic lever. The timing of the muscle length clamp is controlled manually through the adjustment of a programmable timer triggered by a muscle stimulator pulse. This method has an advantage, in that the instant of the length clamp can be adjusted independently of muscle force and muscle length, and a disadvantage, in that it is feasible only during stable twitches. The disadvantage is the reason we employed the fully isometric twitch for the evaluation of inotropic interventions on relaxation characteristics. The third method, which was described in detail in our previous report (16), requires two mechanical stoppers called the end-diastolic and end-systolic stoppers combined with metal contact. In this method, muscle displacement itself cyclically switches the level of iso-

tonic load at the moments of the minimum and maximum muscle length. This method has an advantage, in that the isotonic relengthening at preload can easily be realized and a disadvantage, in addition to that of the first method, in that the onset of the isometric relaxation phase begins essentially before the instant of the shortest muscle length. The fourth method, which utilized a computer-based force servo system (13, 19, 20), is the most sophisticated and feasible, even when contraction is unstable. The trigger signal that switches servo mode from isotonic to isometric and vice versa is generated through muscle length and muscle force measurement. This method has a disadvantage, in that the servo-mode switch occurs essentially after the instant of the shortest muscle length, because the instant of minimum muscle length can be identified after the muscle begins to relengthen. Examination of the study on skeletal muscle relaxation (7) and the force traces of our own preliminary experiments led us to conclude that an initial concave isometric force decline should be ascribed to an inappropriate timing of the muscle length clamp. The premature length clamp in the way of the isotonic shortening produces a force redevelopment exceeding the preceding isotonic load. In the experiment of physiologically sequenced contraction employing the third method, the length clamp should occur a few milliseconds after the muscle attains its shortest length. This delayed switch occasionally produces a distinct discontinuity in force trace (Fig. 4 in Ref. 20). If this is the case, the contour of the isometric relaxation resembles that of the conventional isotonic afterloaded contraction (Fig. 4, trace b, in Ref. 7). In the current

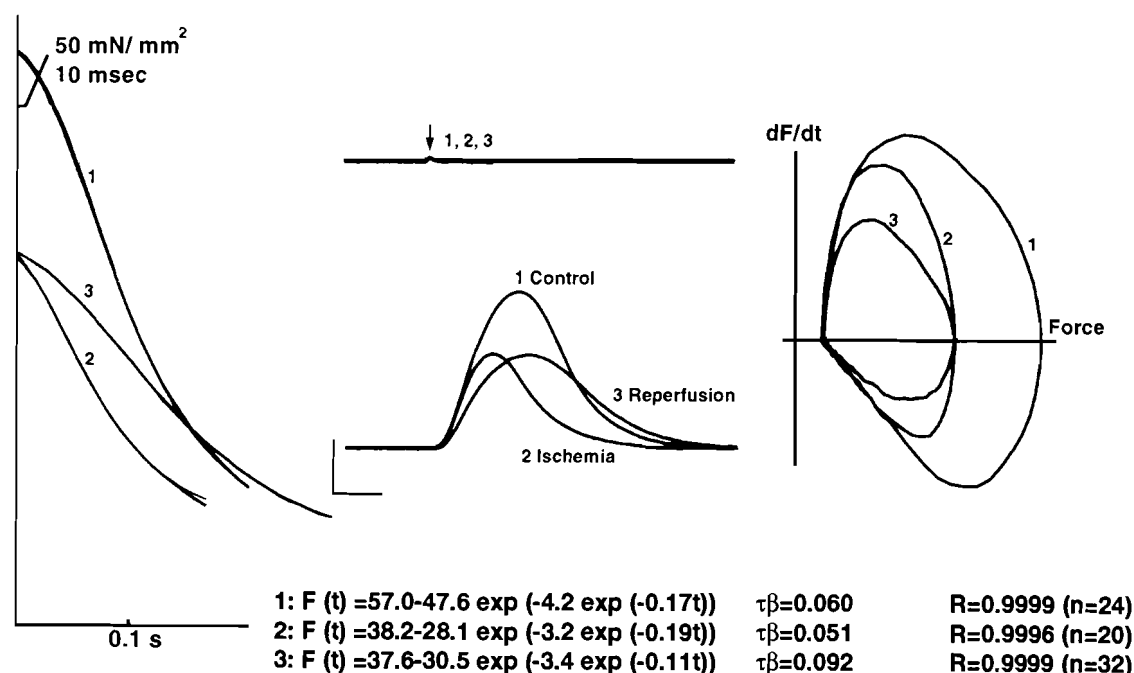


Fig. 10. Representative traces of fully isometric twitches before, during, and after global ischemia for 90 s. See legends to Figs. 4 and 6 for details. Global ischemia curtailed time required for its peak force and  $\tau\beta$ , and reperfusion prolonged both. During reperfusion,  $\alpha$  does not increase, possibly because of inappropriate identification of relaxation onset due to broadened peak of muscle force.

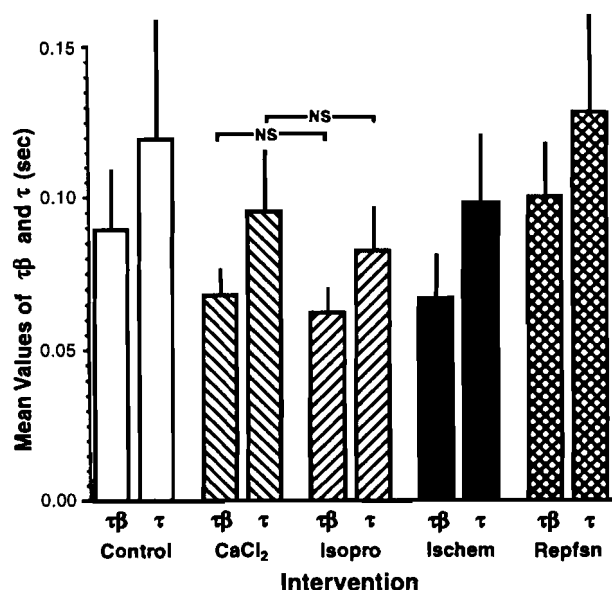


Fig. 11. Changes in  $\tau_\beta$  and  $\tau$  during interventions of  $\text{CaCl}_2$  (bolus infusion of 0.5 mg), isoproterenol (bolus infusion of 0.025  $\mu\text{g}$ ), global ischemia (90 s), and subsequent reperfusion ( $\sim 30$  s after onset of reperfusion) in isometric twitch. Statistical significance was found among all combinations except those indicated as NS (ANOVA with Bonferroni's multiple comparison,  $P < 0.01$ ). Vertical bars, SD.

study, the timing of the muscle length clamp was carefully adjusted for the smooth transition in force. Accordingly, the force recording in the isometric relaxation phase always started convexly with zero slope and then declined concavely even at a very low level of isotonic load.

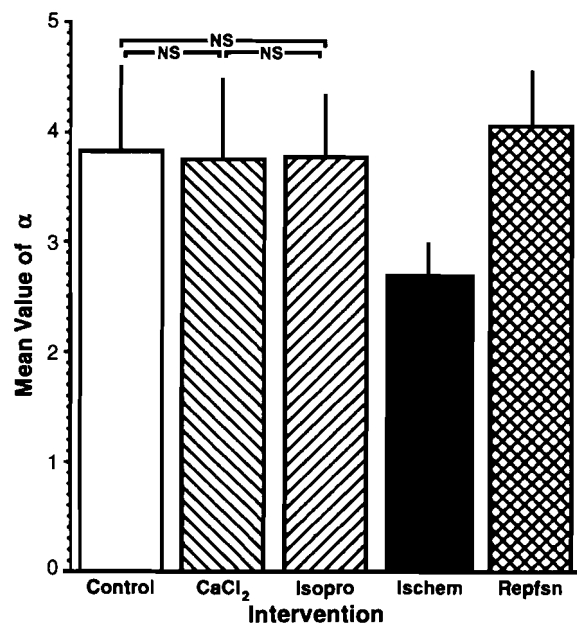


Fig. 12. Changes in  $\alpha$  during interventions of  $\text{CaCl}_2$ , isoproterenol, global ischemia, and subsequent reperfusion in isometric twitch. See legend to Fig. 11 for details. Statistical significance was found among all combinations except those indicated as NS (ANOVA with Bonferroni's multiple comparison,  $P < 0.01$ ).

Because of the higher correlation coefficient and reproducibility of the double-exponential curve fitting, one may anticipate that it implies some underlying mechanism that regulates myocardial relaxation. However, it is unclear why the time course of isometric force decline mimics the double-exponential function. The double-exponential function was originally proposed as a mathematical notation of the stochastic process between death rate and age in a single human population and is independent of individual cause of death. We postulated an analogy between death rate and a fraction of the cross-bridges being inactivated in the time course of muscle relaxation. As a speculation, irrespective of how and why an individual cross-bridge is inactivated, global behavior of the residual cross-bridge linkage might fit with the stochastic expression. One may wonder if the initial convexity in muscle force decay should originate from differences in the relaxation onset across the muscle, and a single fiber still relaxes monoexponentially just after the abrupt onset of relaxation. A single muscle fiber contains numerous cross-bridges, and the development of force (activation) in a single cross-bridge might be quantized. No information on how a single cross-bridge develops and conceals its tension-bearing ability is available, and the evidence of a new biochemical process that actualizes relaxation was not reported in the time course of systole and diastole. Myocardial relaxation rather seems to be governed by a balance between activation initiated by the muscle stimulation and continuing inactivation of the cross-bridges. Admittedly, the rate of force decline is dependent on the instantaneous muscle force; i.e., the higher the force at which the muscle begins to relax, the faster the muscle force declines (15). On the other hand, higher isotonic load (smaller amount of muscle shortening) shifts the instantaneous force vs. rate of force relation rightward, as demonstrated in Fig. 6. In both contexts, myocardial relaxation is load dependent (2). Myocardial contraction (force development, displacement against force) is also a function of mechanical loads and is load dependent as well. Hence, it seems unfair to emphasize the load dependence of myocardial relaxation only. The parametric expression proposed here is expected to represent the load-independent "myocardial relaxability," which will be a conceptual counterpart of the "myocardial contractility." The effects of mechanical load alteration and inotropic interventions on  $\alpha$ , which is expected to represent the phasic delay of the relaxation onset, were not thoroughly explored in the present study because of the ambiguous definition of the isometric relaxation onset in the physiologically sequenced relaxation. One may consider that the muscle stimulation should be the time reference for measuring the delay of myocardial relaxation onset. However, there is no means to distinguish the retardation of contraction from the delay of relaxation onset. In the current study, the effects of changes in contraction frequency on the relaxation indexes under various modes of contraction-relaxation sequence were not explored and were left for further investigation. Finally, because

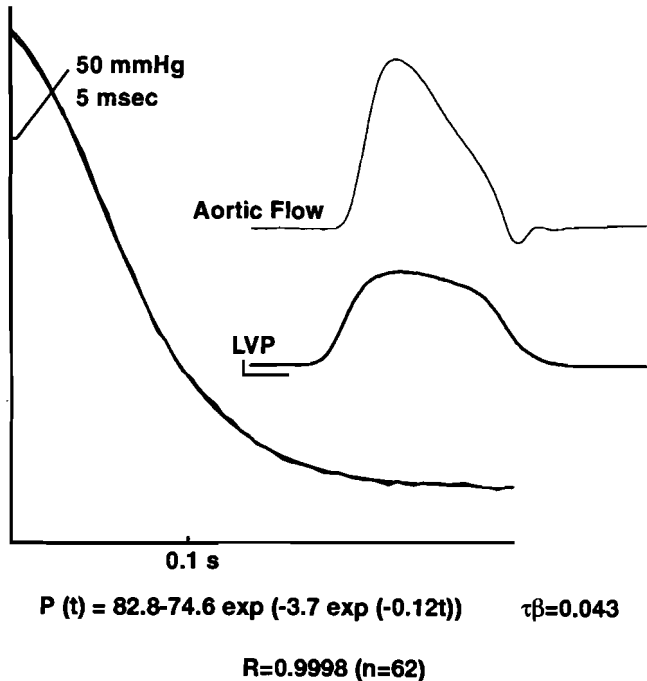


Fig. 13. Representative double-exponential curve fitting to isovolumic left ventricular pressure fall of a dog. *Left*: bold line, isovolumic pressure fall; fine line, its double-exponential regression curve. *Right*: fine line, aortic flow; bold line, left ventricular pressure (LVP). A small right angle denotes 10-mmHg pressure scale (vertical bar) and 0.1-s time scale (horizontal bar). *Bottom*: regression equation. Unit of  $\tau\beta$  is s.

of the unique linear relation between wall stress and intraventricular pressure during the isovolumic relaxation phase, one may expect to apply the present method to the normally ejecting ventricle. Figure 13 shows a sample double-exponential curve fitting to the left ventricular pressure trace from an anesthetized open-chest dog. The time course of the left ventricular pressure fall was a good fit with Gompertz's double-exponential curve as well as the isometric force decay in the papillary muscle preparation unless it was recorded near the aortic valve, except  $\tau\beta$  was obviously shorter in the ventricle than in the isolated myocardium.

In conclusion, the new load-independent parameters of myocardial lusitropism,  $\alpha$  and  $\tau\beta$ , were proposed in the physiologically sequenced relaxation and in the fully isometric twitch.  $\text{CaCl}_2$ , isoproterenol, and global ischemia facilitated relaxation in terms of curtailment of  $\tau\beta$ , whereas subsequent reperfusion prolonged it. Only the global ischemia and subsequent reperfusion affected  $\alpha$  in the fully isometric twitch, suggesting the capability to discriminate the effect of ischemia on the lusitropic state from the effect of inotropic interventions through the present evaluation method. Load-independent assessment of the myocardial lusitropic state in the whole heart during the isovolumic relaxation phase is promising utilizing the current method.

#### APPENDIX A

Let the pairs of time  $t$  and the logarithmic value of muscle force  $\ln[F(t)]$  be divided into three groups of equal quantity

( $t = 1, \dots, n-1, n, \dots, 2n-1, 2n, \dots, 3n-1$ ), as noted below. One or two data pairs in excess of a multiple of three are discarded.

	group 1	group 2	group 3
$t$	$1, 2, \dots, n-1$	$n, n+1, \dots, 2n-1$	$2n, 2n+1, \dots, 3n-1$
$\ln F(t)$	$F_1, F_2, \dots, F_{n-1}$	$F_n, F_{n+1}, \dots, F_{2n-1}$	$F_{2n}, F_{2n+1}, \dots, F_{3n-1}$

We substitute  $K$  for  $\ln(\gamma)$ ,  $a$  for  $\alpha$ , and  $b$  for  $\exp(-\beta)$ . Gompertz's equation  $F(t) = \gamma \cdot \exp[-\alpha \cdot \exp(-\beta t)]$  can be written as

$$\ln[F(t)] = K - ab^t \quad (A1)$$

The sum of  $\ln[F(t)]$  within each individual group is  $S_1$ ,  $S_2$ , and  $S_3$ , respectively.  $S_1$ ,  $S_2$ , and  $S_3$  are written as

$$\begin{aligned} S_1 &= \sum_{t=0}^{n-1} \ln[F(t)] = \sum_{t=0}^{n-1} (K - ab^t) \\ &= nK - (a + ab + \dots + ab^{n-1}) \end{aligned} \quad (A2)$$

$$= nK - a(1 + b + \dots + b^{n-1})$$

$$= nK - a[(b^n - 1)/(b - 1)]$$

$$\begin{aligned} S_2 &= \sum_{t=n}^{2n-1} \ln[F(t)] = \sum_{t=n}^{2n-1} (K - ab^t) \\ &= nK - (ab^n + ab^{n+1} + \dots + ab^{2n-1}) \end{aligned} \quad (A3)$$

$$= nK - ab^n(1 + b + \dots + b^{n-1})$$

$$= nK - ab^n[(b^n - 1)/(b - 1)]$$

$$\begin{aligned} S_3 &= \sum_{t=2n}^{3n-1} \ln[F(t)] = \sum_{t=2n}^{3n-1} (K - ab^t) \\ &= nK - (ab^{2n} + ab^{2n+1} + \dots + ab^{3n-1}) \\ &= nK - ab^{2n}(1 + b + \dots + b^{n-1}) \\ &= nK - ab^{2n}[(b^n - 1)/(b - 1)] \end{aligned} \quad (A4)$$

According to Eqs. A2–A4

$$\begin{aligned} S_2 - S_1 &= nK - ab^n[(b^n - 1)/(b - 1)] - [nK - a(b^n - 1)/(b - 1)] \\ &= [(b^n - 1)/(b - 1)] \cdot a \cdot (1 - b^n) \\ &= -a[(b^n - 1)^2/(b - 1)] \end{aligned} \quad (A5)$$

$$\begin{aligned} S_3 - S_2 &= nK - ab^{2n}[(b^n - 1)/(b - 1)] \\ &\quad - [nK - ab^n(b^n - 1)/(b - 1)] \\ &= [(b^n - 1)/(b - 1)] \cdot ab^n \cdot (1 - b^n) \\ &= -ab^n[(b^n - 1)^2/(b - 1)] \end{aligned} \quad (A6)$$

Dividing Eq. A6 by Eq. A5 yields

$$(S_3 - S_2)/(S_2 - S_1) = b^n \quad (A7)$$

From Eq. A7 we obtain

$$b = [(S_3 - S_2)/(S_2 - S_1)]^{1/n} \quad (A8)$$

Substitution of  $b$  in Eq. A5 for Eq. A8 results in

$$a = (S_1 - S_2)(b - 1)/(b^n - 1)^2 \quad (A9)$$

Equation A2 is written as

$$K = \left[ S_1 + \frac{a(b^n - 1)}{(b - 1)} \right] / n$$

Substitution of  $a$  in this equation for Eq. A9 gives

$$K = \left[ S_1 + \frac{(S_1 - S_2)}{(b^n - 1)} \right] / n$$

Because  $b^n - 1 = [(S_3 - S_2)/(S_2 - S_1)] - 1$  from Eq. A8

$$K = [(S_1 S_3 - S_2^2)/(S_1 - 2S_2 + S_3)]/n \quad (A10)$$

Hence, we obtain values of  $\alpha = a$ ,  $\beta = -\ln(b)$ , and  $\gamma = \exp(K)$  from the values of  $S_1$ ,  $S_2$ ,  $S_3$ , and  $n$  (quantity of the data pairs in the divided group). The  $\gamma_0$  is determined through iteration. Let the upper asymptote  $\gamma_0$  be the maximum muscle stress at first; then the calculation of the regression equation was repeated increasing  $\gamma_0$  stepwise until the sum of square error reached its minimum.  $\gamma_0 - \gamma$  yields the lower asymptote. Thus the four parameters,  $\alpha$ ,  $\beta$ ,  $\gamma$ , and  $\gamma_0$ , of the modified double-exponential equation that yields instantaneous muscle force during the isometric relaxation phase are obtained as follows

$$F(t) = \gamma_0 - \gamma \cdot \exp[-\alpha \cdot \exp(-\beta t)] \quad (A11)$$

## APPENDIX B

Let the force being inactivated during the isometric relaxation phase be  $Y(t)$ .  $Y(t)$  is given as

$$Y(t) = \gamma_0 - F(t) = \gamma \cdot \exp[-\alpha \cdot \exp(-\beta t)] \quad (B1)$$

Then we transform it into a logarithm

$$\alpha \cdot \exp(-\beta t) = \ln \gamma - \ln[Y(t)] \quad (B2)$$

Because  $\ln(\gamma)$  is a constant, the first derivative of Eq. B2 with respect to time  $t$  is written as

$$-dY(t)/dt = -\alpha\beta \cdot \exp(-\beta t) \cdot Y(t) \quad (B3)$$

Substitution of Eq. B2 for  $\alpha \cdot \exp(-\beta t)$  in Eq. B3 yields

$$-dY(t)/dt = -\beta \cdot Y(t) \cdot [\ln(\gamma) - \ln[Y(t)]] \quad (B4)$$

Substitution of Eq. B1 for  $Y(t)$  in Eq. B4 gives

$$-d[\gamma_0 - F(t)]/dt = dF(t)/dt = -\beta \cdot [\gamma_0 - F(t)] \cdot [\ln \gamma - \ln[\gamma_0 - F(t)]] \quad (B5)$$

Equation B5 does not explicitly contain  $t$  and shows that the  $F(t)$  vs.  $dF(t)/dt$  relation (phase-plane diagram) is defined by  $\beta$ ,  $\gamma$ , and  $\gamma_0$ , irrespective of  $\alpha$ .

In the phase-plane diagram [ $F(t)$  vs.  $dF(t)/dt$  trajectory],  $F(t)$  approaches  $\gamma_0 - \gamma$  when  $t$  approaches infinity. The slope of the phase-plane diagram is given as

$$\frac{dF(t)/dt}{F(t) - (\gamma_0 - \gamma)} = \frac{-\beta[\gamma_0 - F(t)] \cdot [\ln \gamma - \ln[\gamma_0 - F(t)]]}{F(t) - (\gamma_0 - \gamma)} \quad (B6)$$

When the numerator and denominator are divided by  $\gamma_0 - F(t)$ , the limit value of Eq. B6 is

$$\lim_{t \rightarrow \infty} \frac{dF(t)/dt}{F(t) - (\gamma_0 - \gamma)} = \lim_{t \rightarrow \infty} -\beta \cdot \frac{\ln[\gamma/[\gamma_0 - F(t)]]}{[\gamma/[\gamma_0 - F(t)]] - 1}$$

With use of  $X$  for  $[\gamma/[\gamma_0 - F(t)]] - 1$  and Taylor's expansion for  $\ln(1 + X)$

$$\begin{aligned} \lim_{X \rightarrow 0} -\beta \cdot \frac{\ln(1 + X)}{X} &= \lim_{X \rightarrow 0} -\beta \cdot \frac{X - X^2/2 + \dots}{X} \\ &= \lim_{X \rightarrow 0} -\beta \left( 1 - \frac{X}{2} + \frac{X^2}{3} - \dots \right) = -\beta \end{aligned} \quad (B7)$$

Equation B7 reveals that the terminal slope of the phase-plane diagram of the double-exponential curve is determined by  $\beta$  alone.

Differentiation of Eq. B3 again with respect to time  $t$  yields

$$d^2Y(t)/dt^2 = -\alpha\beta^2 \cdot \exp(-\beta t) \cdot Y(t) + \alpha\beta \cdot \exp(-\beta t) \cdot dY(t)/dt$$

Substitution of Eq. B3 for  $dY(t)/dt$  in this equation gives

$$\begin{aligned} d^2Y(t)/dt^2 &= -\alpha\beta^2 \cdot \exp(-\beta t) \cdot Y(t) + \alpha^2\beta^2 \cdot \exp^2(-\beta t) \cdot Y(t) \\ &= -\alpha\beta^2 \cdot \exp(-\beta t) \cdot Y(t) \cdot [1 - \alpha \cdot \exp(-\beta t)] \end{aligned} \quad (B8)$$

Because  $\gamma_0$  is a constant, the first derivative of  $F(t)$  with respect to time has its peak [an inflection point in  $F(t)$ ] when  $\alpha \cdot \exp(-\beta t) = 1$ , i.e.,  $t = \ln(\alpha/\beta)$ . With substitution of  $Y(t)$  in Eq. B3 for  $\gamma_0 - F(t)$ , the peak rate of force decay is given as

$$d[\gamma_0 - F(t)]/dt_{\max} = \alpha\beta \cdot \exp(-\beta t) \cdot [\gamma_0 - F(t)]$$

Substitution of  $\alpha \cdot \exp(-\beta t) = 1$  in this equation gives

$$\begin{aligned} dF(t)/dt_{\max} &= -\beta \cdot [\gamma_0 - F(t)] \\ &= -\beta \cdot \gamma_0 + \beta[\gamma_0 - \gamma \cdot \exp[-\alpha \cdot \exp(-\beta t)]] \\ &= -\beta\gamma \cdot \exp(-1) \end{aligned} \quad (B9)$$

Thus peak negative  $dF(t)/dt$  is directly related to the values of  $\beta$  and  $\gamma$  independently of  $\alpha$  and  $\gamma_0$ , and the terminal slope of the  $F(t)$  vs.  $dF(t)/dt$  relation equals  $-\beta$ .

Address for reprint requests: K. Tamiya, Dept. of Internal Medicine, Douaikai Hospital, 1-42-21 Matsushima, Edogawa-ku, Tokyo 132, Japan.

Received 2 June 1994; accepted in final form 27 January 1995.

## REFERENCES

1. Bing, O. H. L., J. F. Keefe, M. J. Wolk, L. J. Finkelstein, and H. J. Levine. Tension prolongation during recovery from myocardial hypoxia. *J. Clin. Invest.* 50: 660-666, 1971.

2. **Brutsaert, D. L., and S. U. Sys.** Relaxation and diastole of the heart. *Physiol. Rev.* 69: 1228–1315, 1989.
3. **Endoh, M., and K. Hashimoto.** Pharmacological evidence of autonomic nerve activities in canine papillary muscle. *Am. J. Physiol.* 218: 1459–1463, 1970.
4. **Frederiksen, J. W., J. L. Weiss, and M. L. Weisfeldt.** Time constant of isovolumic pressure fall: determinants in the working left ventricle. *Am. J. Physiol.* 235 (Heart Circ. Physiol. 4): H701–H706, 1978.
5. **Goethals, M. A., P. R. Housmans, and D. L. Brutsaert.** Load-dependence of physiologically relaxing cardiac muscle. *Eur. Heart J.* 1: 81–87, 1980.
6. **Goethals, M. A., P. R. Housmans, and D. L. Brutsaert.** Loading determinants of relaxation in cat papillary muscle. *Am. J. Physiol.* 242 (Heart Circ. Physiol. 11): H303–H309, 1982.
7. **Jewell, B. R., and D. R. Wilkie.** The mechanical properties of relaxing muscle. *J. Physiol. Lond.* 152: 30–47, 1960.
8. **Karliner, J. S., M. M. LeWinter, F. Mahler, R. Engler, and R. A. O'Rourke.** Pharmacologic and hemodynamic influences on the rate of isovolumic left ventricular relaxation in the normal conscious dog. *J. Clin. Invest.* 60: 511–521, 1977.
9. **Le Carpentier, Y. C., L. H. S. Chuck, P. R. Housmans, N. M. DeClerck, and D. L. Brutsaert.** Nature of load dependence of relaxation in cardiac muscle. *Am. J. Physiol.* 237 (Heart Circ. Physiol. 6): H455–H460, 1979.
10. **Nwasokwa, O. N., and M. M. Bodenheimer.** Analysis of myocardial isometric dynamics using parameters of a global model. *Am. J. Physiol.* 257 (Heart Circ. Physiol. 26): H1275–H1286, 1989.
11. **Parmley, W. W., and E. H. Sonnenblick.** Relation between mechanics of contraction and relaxation in mammalian cardiac muscle. *Am. J. Physiol.* 216: 1084–1091, 1969.
12. **Sabbah, H. N., and P. D. Stein.** Investigation of the theory and mechanisms of the origin of the second heart sound. *Circ. Res.* 39: 874–882, 1976.
13. **Sulman, D. L., O. H. L. Bing, R. G. Mark, and S. K. Burns.** Physiologic loading of isolated heart muscle. *Biochem. Biophys. Res. Commun.* 56: 947–951, 1974.
14. **Sys, S. U., and D. L. Brutsaert.** Determinants of force decline during relaxation in isolated cardiac muscle. *Am. J. Physiol.* 257 (Heart Circ. Physiol. 26): H1490–H1497, 1989.
15. **Tamiya, K., S. Kikkawa, M. Gunji, and M. Hori.** Maximum rate of tension fall during isometric relaxation at end-systolic fiber length in canine papillary muscle. *Circ. Res.* 40: 584–589, 1977.
16. **Tamiya, K., M. Sugawara, and Y. Sakurai.** Maximum lengthening velocity during isotonic relaxation at preload in canine papillary muscle. *Am. J. Physiol.* 237 (Heart Circ. Physiol. 6): H83–H89, 1979.
17. **Wallenstein, S., C. L. Zucker, and J. L. Fleiss.** Some statistical methods useful in circulation research. *Circ. Res.* 47: 1–9, 1980.
18. **Weiss, J. L., J. W. Frederiksen, and M. L. Weisfeldt.** Hemodynamic determinants of the time-course of fall in canine left ventricular pressure. *J. Clin. Invest.* 58: 751–760, 1976.
19. **Wiegner, A. W., and O. H. L. Bing.** Isometric relaxation of rat myocardium at end-systolic fiber length. *Circ. Res.* 43: 865–869, 1978.
20. **Zile, M. R., C. H. Conrad, W. H. Gaash, K. G. Robinson, and O. H. L. Bing.** Preload does not affect relaxation rate in normal, hypoxic, or hypertrophic myocardium. *Am. J. Physiol.* 258 (Heart Circ. Physiol. 27): H191–H197, 1990.